SINTEF
PROCEEDINGS
2

Proceedings of the 12th International Conference on Computational Fluid Dynamics in the Oil & Gas, Metallurgical and Process Industries

Progress in Applied CFD – CFD2017

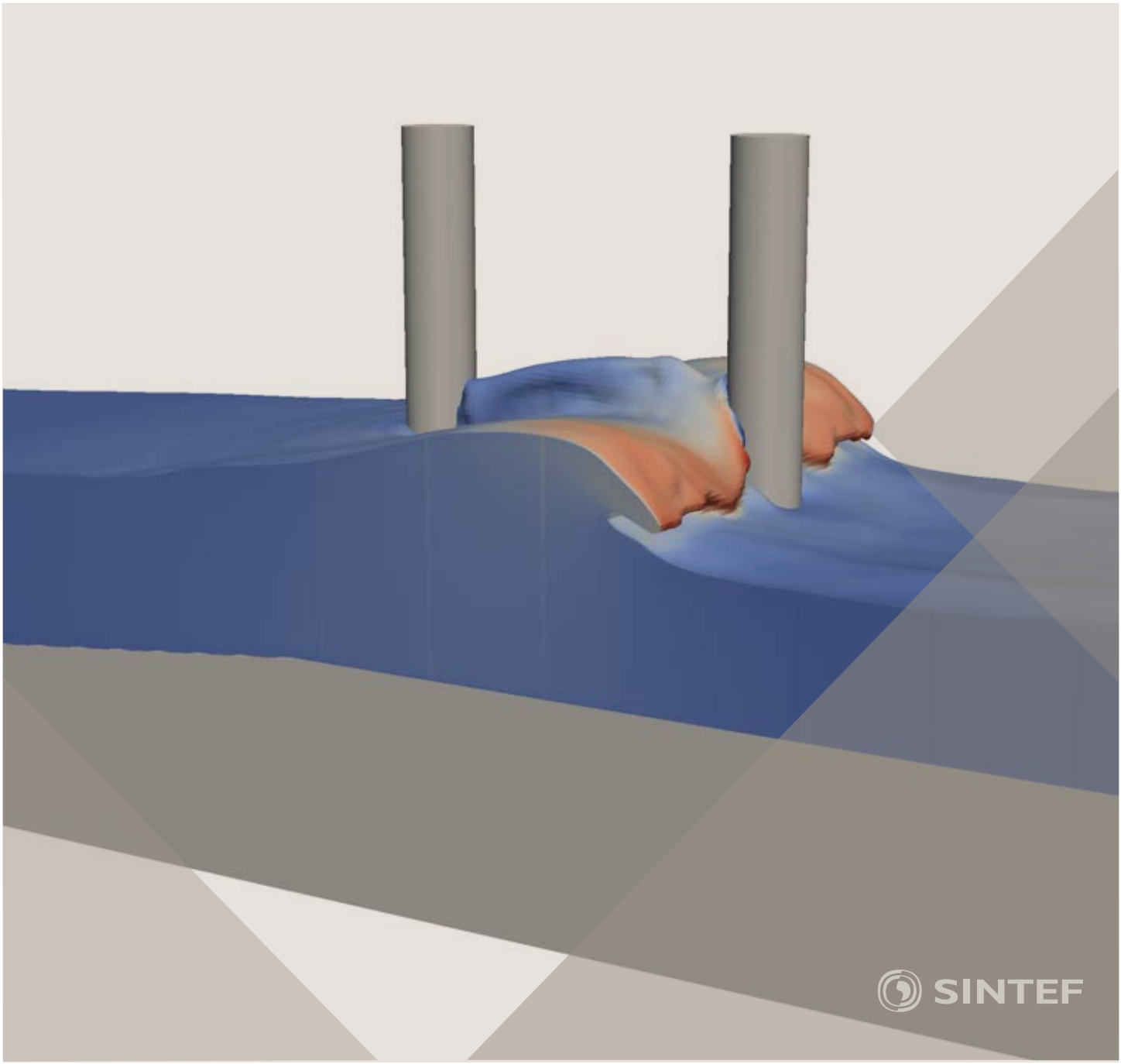

SINTEF Proceedings

Editors:
Jan Erik Olsen and Stein Tore Johansen

Progress in Applied CFD – CFD2017

Proceedings of the 12th International Conference on Computational Fluid Dynamics in the Oil & Gas, Metallurgical and Process Industries

SINTEF Academic Press

SINTEF Proceedings no 2
Editors: Jan Erik Olsen and Stein Tore Johansen
Progress in Applied CFD – CFD2017
Selected papers from 10th International Conference on Computational Fluid Dynamics in the Oil & Gas, Metallurgical and Process Industries

Key words:
CFD, Flow, Modelling

Cover, illustration: Arun Kamath

ISSN 2387-4295 (online)
ISBN 978-82-536-1544-8 (pdf)

SINTEF Academic Press
Address: Forskningsveien 3 B
PO Box 124 Blindern
N-0314 OSLO
Tel: +47 73 59 30 00
Fax: +47 22 96 55 08

www.sintef.no/byggforsk
www.sintefbok.no

SINTEF Proceedings
SINTEF Proceedings is a serial publication for peer-reviewed conference proceedings on a variety of scientific topics.
The processes of peer-reviewing of papers published in SINTEF Proceedings are administered by the conference organizers and proceedings editors. Detailed procedures will vary according to custom and practice in each scientific community.

PREFACE

This book contains all manuscripts approved by the reviewers and the organizing committee of the 12th International Conference on Computational Fluid Dynamics in the Oil & Gas, Metallurgical and Process Industries. The conference was hosted by SINTEF in Trondheim in May/June 2017 and is also known as CFD2017 for short. The conference series was initiated by CSIRO and Phil Schwarz in 1997. So far the conference has been alternating between CSIRO in Melbourne and SINTEF in Trondheim. The conferences focuses on the application of CFD in the oil and gas industries, metal production, mineral processing, power generation, chemicals and other process industries. In addition pragmatic modelling concepts and bio-mechanical applications have become an important part of the conference. The papers in this book demonstrate the current progress in applied CFD.

The conference papers undergo a review process involving two experts. Only papers accepted by the reviewers are included in the proceedings. 108 contributions were presented at the conference together with six keynote presentations. A majority of these contributions are presented by their manuscript in this collection (a few were granted to present without an accompanying manuscript).

The organizing committee would like to thank everyone who has helped with review of manuscripts, all those who helped to promote the conference and all authors who have submitted scientific contributions. We are also grateful for the support from the conference sponsors: ANSYS, SFI Metal Production and NanoSim.

Stein Tore Johansen & Jan Erik Olsen

Organizing committee:

Conference chairman: Prof. Stein Tore Johansen
Conference coordinator: Dr. Jan Erik Olsen
Dr. Bernhard Müller
Dr.Sigrid Karstad Dahl
Dr.Shahriar Amini
Dr.Ernst Meese
Dr.Josip Zoric
Dr.Jannike Solsvik
Dr.Peter Witt

Scientific committee:

Stein Tore Johansen, SINTEF/NTNU
Bernhard Müller, NTNU
Phil Schwarz, CSIRO
Akio Tomiyama, Kobe University
Hans Kuipers, Eindhoven University of Technology
Jinghai Li, Chinese Academy of Science
Markus Braun, Ansys
Simon Lo, CD-adapco
Patrick Segers, Universiteit Gent
Jiyuan Tu, RMIT
Jos Derksen, University of Aberdeen
Dmitry Eskin, Schlumberger-Doll Research
Pär Jönsson, KTH
Stefan Pirker, Johannes Kepler University
Josip Zoric, SINTEF

CONTENTS

MASS TRANSFER PHENOMENA IN FLUIDIZED BEDS WITH HORIZONTALLY IMMERSED MEMBRANES

Ramon J.W. VONCKEN[1], Ivo ROGHAIR[1]*, Martin VAN SINT ANNALAND[1]

[1] Chemical Process Intensification, Department of Chemical Engineering and Chemistry, Eindhoven University of Technology, THE NETHERLANDS

* Corresponding author e-mail: i.roghair@tue.nl

ABSTRACT

Mass transfer phenomena in fluidized bed reactors with horizontally immersed membranes have been investigated using a verified and validated Two-Fluid Model. A binary hydrogen-nitrogen mixture was injected into the fluidized bed which was operated in the bubbling fluidization regime, and hydrogen was extracted via horizontally immersed membranes. The hydrogen flux is lowest on top of the membranes and highest at the bottom of the membranes. The main causes for the low flux on top of the membranes are densified zones and insufficient hydrogen replenishment due to the flow pattern of the gas. Gas pockets do not have a negative effect on the mass transfer towards the membranes. In systems with membrane tube banks, the membranes located at the walls perform worst, because solids mostly flow downwards near the walls of a fluidized bed, which causes gas back-mixing, which hinders hydrogen replenishment and thereby decreases the driving force for hydrogen transport. Removing the membranes closest to the wall increases the overall efficiency of the system. Replacing wall membranes with inactive tubes has no significant effect on the system. The membrane tube banks also have a significant effect on the hydrodynamics.

Keywords: Two-Fluid Model, mass transfer, hydrodynamics, fluidized bed, membrane.

NOMENCLATURE

Latin Symbols

A	area	[m^2]
C_d	drag coefficient	[-]
D	diffusion coefficient	[m^2/s]
e	restitution coefficient	[-]
g	gravitational acceleration	[m/s^2]
M	molar weight	[kg/mol]
n	power in Sieverts' law	[-]
p	pressure	[Pa]
Q	membrane permeance	[$mol/(m^2.s.Pa^n)$]
R	universal gas constant	[J/(mol.K)]
Re	Reynolds number	[-]
S	membrane mass source term	[$kg/(m^3.s)$]
t	time	[s]
T	temperature	[K]
$\boldsymbol{u}$	velocity	[m/s]
V	volume	[m^3]
X	molar fraction	[-]
Y	mass fraction	[-]

Greek Symbols

α	hold-up fraction	[-]
β	interphase drag coefficient	[$kg/(m^3.s)$]
γ	dissipation of fluctuation energy	[$kg/(m.s^3)$]
θ	granular temperature	[m^2/s^2]
κ	conductivity of fluctuation energy	[kg/(m.s)]
μ	shear/dynamic viscosity	[Pa.s]
ρ	density	[kg/m^3]
$\boldsymbol{\tau}$	shear stress tensor	[N/m^2]

Sub/superscripts

c	cell
H_2	hydrogen
g	gas
i	phase
m	membrane
mf	minimum fluidization
p	particle
ret	retentate
s	solid
sim	simulation
tot	total
w	wall

INTRODUCTION

Hydrogen is commonly produced by Steam Methane Reforming (SMR), which can be performed in (multi-tubular) packed bed reactors. In the packed beds, methane reacts with steam to form carbon monoxide and hydrogen at temperatures around 1000 °C. Consecutively, the Water Gas Shift (WGS) reaction occurs; the carbon monoxide reacts with steam to form carbon dioxide and hydrogen. To ensure a high methane conversion, high temperatures and low hydrogen concentrations are required. Separating the unwanted byproduct CO_2 from the outlet gas mixture requires complex and energy intensive separation units such as pressure swing adsorption columns, and will result in an increase in cost and energy usage, and a decrease in system performance (Medrano et al. (2014)).

A promising new approach to circumvent the drawbacks of the current hydrogen production methods is

integrating the reaction and separation steps in one unit. Extracting hydrogen from the gas mixture with modern, high-flux hydrogen perm-selective palladium membranes purifies the hydrogen whilst simultaneously driving the chemical reaction equilibria towards the product side. The reactor can therefore operate at a lower temperature (600-700 °C) than the industrial process. The integration of hydrogen perm-selective membranes in packed bed reactors has already been investigated by Tsotsis et al. (1992), Tiemersma et al. (2006) and many others.

In packed bed membrane reactor systems, catalyzed reactions and separation of product and waste are performed in the same unit. However, a major drawback of packed bed membrane reactors is the low mixing efficiency, causing temperature and concentration gradients in the reactor. When using state-of-the-art membranes, the system is not limited by the permeation rate, but limited by the mass transfer rate of hydrogen towards the membranes, which is called concentration polarization (Caravella et al. (2009)). To circumvent these drawbacks, fluidized bed membrane reactors have been proposed to extract hydrogen from the reaction mixture, see Adris et al. (1994), Gallucci (2008), Mleczko et al. (1996) and Hommel et al. (2012).

Compared to packed bed membrane reactors, fluidized bed membrane reactors have better mixing properties, resulting in reduced mass transfer limitations towards the membranes. The hydrodynamics and mass transfer phenomena of the fluidized suspension can be strongly affected by the membrane configuration. Possible hydrodynamic consequences of installing membranes in fluidized beds have been demonstrated by e.g. De Jong et al. (2011), Dang et al. (2014), Tan et al. (2014), Wassie et al. (2015) and Medrano et al. (2015). Industrially, membranes immersed in the particle emulsion of a fluidized bed may be damaged due to attrition, so for large scale applications a protective nano-layer coating or a porous filter could be applied to prevent this. Having said this, Helmi et al. (2016) have successfully demonstrated the long term (over 900 hours) performance of a fluidized bed membrane reactor utilizing very high flux membranes for ultra-pure hydrogen production via WGS.

Membranes are mostly inserted vertically in reactors. Helmi et al. (2017) have demonstrated that when using state-of-the-art high-flux palladium membranes to extract hydrogen from a hydrogen/nitrogen gas mixture, mass transfer limitations from the bed to the membrane (concentration polarization) can severely limit the extracted flux. Furthermore, recent experimental findings suggest that vertically immersed membranes hardly affect the gas bubbles that are passing by. By inserting the membranes perpendicular to the flow direction (i.e. horizontally), the membranes can cut large gas bubbles into smaller ones, hereby improving the mixing efficiency of the bed. Previous studies by Medrano et al. (2015), De Jong et al. (2012), Asegehegn et al. (2011), Rong et al. (1999), Solnordal et al. (2015), Wang et al. (2015), Yang et al. (2014) and Sarkar et al. (2013) on horizontal tubes immersed in fluidized beds have already proven that tubes have a significant effect on the bed hydrodynamics. However, very little work has been done on mass transfer phenomena in fluidized bed reactors with horizontally immersed membranes.

This work is a numerical study on the mass transfer phenomena in fluidized bed reactors with horizontally immersed membranes. The goal of this work is to describe, identify and explain the most important mass transfer phenomena occurring in fluidized beds with horizontally immersed membranes. Explaining the mass transfer phenomena will also require relating the observed mass transfer phenomena to the hydrodynamics. For example, Medrano et al. (2015) found that gas pockets (solids free, non-rising gas bubbles) occur underneath and densified particle zones occur on top of horizontally submerged membranes. The gas pockets and densified zones may affect the mass transfer towards the membranes and could therefore have a noticeable effect on the system performance.

Because palladium-based membranes are quite expensive, placing them at locations where they perform sub-optimally should be avoided. Exploratory simulations have already indicated that reduced hydrogen concentrations are mostly found at membranes near the bed walls (see Voncken et al. (2015)), so the performance of these membranes are especially worth investigating. Therefore, we have simulated fluidized beds with various membrane tube bank configurations with and without membranes near the bed walls. However, simply removing membranes near the wall could also affect the solids circulation patterns, the bubble cutting behavior of the tube banks and could induce gas bypassing via the walls, so fluidized beds with inactive tubes instead of membranes near the walls were also simulated.

A Two-Fluid Model (TFM) was used to perform the simulations and to obtain detailed information on the mass transfer phenomena occurring near the membranes. The OpenFOAM v.2.3.0 TFM (*twoPhaseEulerFoam*) was used as hydrodynamic framework, and was extended with a species balance equation and realistic membrane models to simulate selective extraction of hydrogen from the system.

First, the model equations, verification and validation will be discussed. Special attention will be given to the implementation of the species balance, the implementation of the membrane source term and the membrane boundary condition. Next, the simulation settings and the tube bank geometries will be presented. In the results section, the most important mass transfer phenomena and hydrodynamics will be presented and explained.

MODEL DESCRIPTION

A TFM considers the gas and solids phase as interpenetrating continua. The most important governing and constitutive equations are presented in equations 1 through 6. The continuity equations (1) of both gas and solids phase are very similar. The source term S is added to the gas continuity equation to take into account the extraction of gas via membranes. The membrane source term will be presented in the mass transfer and membranes section. Compared to the Navier-Stokes equations of the gas phase (2), the Navier-Stokes equations for the solids phase (3) contain

an additional solids pressure term p_s. For both phases a Newtonian stress tensor $\boldsymbol{\tau}$ is employed. The gas phase density is described with the ideal gas law. Furthermore, the granular temperature equation (4) is solved. The granular temperature equation incorporates the mean particle velocity and a superimposed fluctuating component, taking into account the vibrations of particles due to collisions.

$$\frac{\partial(\alpha_i\rho_i)}{\partial t}+\nabla\cdot(\alpha_i\rho_i\mathbf{u}_i)=S_m,\quad \mathrm{i}=\mathrm{s,g} \tag{1}$$

$$\frac{\partial(\alpha_g\rho_g\mathbf{u}_g)}{\partial t}+\nabla\cdot(\alpha_g\rho_g\mathbf{u}_g\mathbf{u}_g) = -\nabla\cdot(\alpha_g\boldsymbol{\tau}_g)-\alpha_g\nabla p-\beta\cdot(\mathbf{u}_g-\mathbf{u}_s)+\alpha_g\rho_g\mathbf{g} \tag{2}$$

$$\frac{\partial(\alpha_s\rho_s\mathbf{u}_s)}{\partial t}+\nabla\cdot(\alpha_s\rho_s\mathbf{u}_s\mathbf{u}_s)=-\nabla\cdot(\alpha_s\boldsymbol{\tau}_s) -\alpha_s\nabla p-\nabla p_s+\beta\cdot(\mathbf{u}_g-\mathbf{u}_s)+\alpha_s\rho_s\mathbf{g} \tag{3}$$

$$\frac{3}{2}\left(\frac{\partial(\alpha_s\rho_s\theta)}{\partial t}+\nabla\cdot(\alpha_s\rho_s\mathbf{u}_s\theta)\right)=-\gamma_s-3\beta\theta -(p_s\boldsymbol{I}+\alpha_s\boldsymbol{\tau}_s):\nabla\mathbf{u}_s+\nabla\cdot(\alpha_s\kappa_s\nabla\theta) \tag{4}$$

The drag between the solids and the gas phase is modelled according to Gidaspow (1994), which combines the drag model of Ergun et al. (1949) and Wen et al. (1966). Ergun's model is valid for high solids hold-ups (20% and higher) and Wen's model is valid at lower solids hold-ups (below 20%). The drag coefficient C_d is determined based on the Reynolds particle number. The drag models are described in equations 5 until 9.

$$\beta=150\frac{\alpha_s^2\mu_g}{\alpha_g d_p^2}+1.75\frac{\alpha_s\rho_g|\mathbf{u}_g-\mathbf{u}_s|}{d_p}\quad(\alpha_s\geq 0.20) \tag{5}$$

$$\beta=\frac{3}{4}C_d\frac{\alpha_g\alpha_s\rho_g}{d_p}|\mathbf{u}_g-\mathbf{u}_s|\alpha_g^{-2.65}\quad(\alpha_s<0.20) \tag{6}$$

$$C_d=\frac{24}{\mathrm{Re}_p}\left(1+0.15\,\mathrm{Re}_p^{0.687}\right)\quad\text{for }\mathrm{Re}_p\leq 1000 \tag{7}$$

$$C_d=0.44\quad\text{for }\mathrm{Re}_p>1000 \tag{8}$$

$$\mathrm{Re}_p=\alpha_g\frac{\rho_g d_p|\mathbf{u}_g-\mathbf{u}_s|}{\mu_g} \tag{9}$$

Kinetic Theory of Granular Flow

To simulate the rheological and collisional properties of the solids phase's continuum approximation more realistically, various KTGF closure equations are required. The closure equations used in this work are presented in **Table 1**. Further details on the TFM-KTGF can be found a.o. in Lun et al. (1984), Kuipers et al. (1992), Gidaspow (1994), Van Wachem (2000), Rusche (2003) and Van Der Hoef et al. (2006). Details on the OpenFOAM TFM can be found in Passalacqua et al. (2011) and Liu et al. (2014).

Table 1: KTGF closures used for TFM simulations.

Quantity	Closure
Solids shear viscosity	Nieuwland et al. (1996)
Solids bulk viscosity	Lun et al. (1984)
Solids pressure	Lun et al. (1984)
Frictional stress	Srivastava & Sundaresan (2003)
Conductivity of fluct. energy	Nieuwland et al. (1996)
Radial distribution function	Ma & Ahmadi (1984)
Dissipation of gran. energy	Nieuwland et al. (1996)

Mass transfer and membranes

Mass transfer phenomena and hydrogen extraction via membranes was modeled similar to the approach of Coroneo et al. (2009). A hydrogen mass balance with Fickian diffusion was added to the model. The mass balance is a transient convection-diffusion equation as shown in equation 10. The diffusion coefficient can have a significant effect on the hydrogen flux. The selective extraction of hydrogen via the membranes was taken into account via the source term, S_m, which is applied to the computational cells adjacent to a membrane boundary (the red cells in **Figure 1**). The source term in equation 10 is the membrane flux calculated with Sieverts' law, multiplied by the boundary cell's area A_c, divided by the cell volume V_c, see equation 11.

$$\frac{\partial\alpha_g\rho_g Y_{H_2}}{\partial t}+\nabla\cdot(\alpha_g\rho_g\mathbf{u}_g Y_{H_2}) =\nabla\cdot(\alpha_g\rho_g D_{H_2}\nabla Y_{H_2})+S_m \tag{10}$$

$$S_m=\frac{A_c}{V_c}Q_m M_{H_2}\cdot\left[\left(X_{H_2}^{ret}p_{tot}\right)^n-\left(X_{H_2}^{perm}p_{tot}\right)^n\right] \tag{11}$$

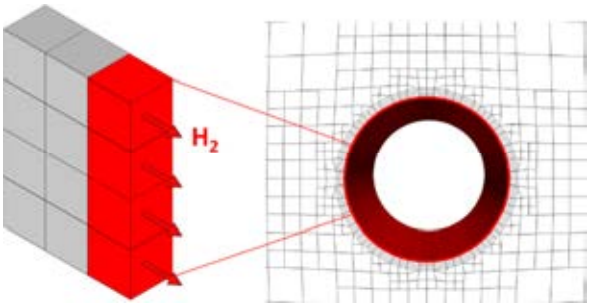

Figure 1: Schematic representation of how and where the membrane source term has been implemented in the grid.

The extraction of mass via a membrane will also result in momentum extraction from the system. Therefore, a boundary condition was added for the membranes to ensure momentum leaves the system. The momentum flux is based on the magnitude of the extractive flux. The boundary condition ultimately imposes a velocity normal to the membrane boundary (see equation 12). For fluidized beds momentum extraction could be an

important topic, because the it can cause densified zones to form near the membranes. Extracting a large amount of the momentum from a fluidized bed can even alter the flow pattern of the solids, as shown by De Jong et al. (2012) and Dang et al. (2014). The work of Helmi et al. (2017) has shown that selective extraction of hydrogen has an effect on the bed hydrodynamics, but that this effect is relatively small.

$$u_m = \frac{S_m RT}{pM_{H_2}} \frac{V_c}{A_c} \tag{12}$$

Boundary conditions

All simulations have been performed with a 2D computational domain. For the gas mixture, a no-slip boundary condition was applied to the left and right walls, a constant gas velocity was imposed at the inlet, an imposed pressure condition was set at the outlet and the boundary condition of equation 12 was applied at the membranes. For the solids velocity and granular temperature, a Johnson & Jackson partial slip boundary condition with a specularity coefficient of 0.50 was applied on the walls and membranes (see Johnson et al. (1987)).

Numerical schemes and accuracy

The temporal discretization was done with the second order Crank-Nicolson scheme. All simulations were run with an adjustable time-step, with a maximum time-step of $1{\cdot}10^{-5}$ s. The selected time-step value each iteration was selected based on a maximum Courant number of 0.1. A combination the second order Gauss linear and Van Leer scheme were used for spatial discretization. The numerical tolerances for the residuals were set to $1{\cdot}10^{-11}$ for each quantity.

VERIFICATION, VALIDATION, GEOMETRIES AND SETTINGS

Verification and validation

The fluid, solid and mass transfer part of the TFM have all been verified and validated. The fluid part of the model has been verified by comparing gas flow profiles, convection and diffusion of a chemical specie to their respective analytical solutions. Gas flow profiles and the pressure drop in a flat rectangular column (pseudo 2D) match very well with the analytical solution of White et al. (1991), even for very coarse grids. Furthermore, combined convection-diffusion of a specie were compared to the analytical solution found in Mohsen et al. (1983). Especially at finer grids and time-steps of 0.001 s and below, the TFM results match well with the analytical solution and the numerical diffusion decreases significantly.

Helmi et al. (2017) have used this TFM to simulate an experimental reactor with one vertically immersed membrane in the center. The TFM was able to predict the experimental fluxes very well and proved to be a useful tool to determine concentration profiles in fluidized bed membrane reactors.

The model was also validated by comparing experimental bubble properties to the simulated ones. The bubble properties match well with experimental bubble diameter and velocity data obtained via Digital Image Analysis of thousands of gas bubbles.

The accuracy of the model for densely packed systems is important because densified zones are expected to occur frequently in fluidized bed membrane reactors, especially on top of the membranes and near the walls. Therefore, the predicted TFM pressure drop over a pseudo 2D packed bed injected with air (ρ_g=1.2 kg/m^3, μ_g=1.84.10^{-5} Pa·s) was compared to the Ergun equation and experimental pressure drop data for 500 µm particles with a density of 2500 kg/m^3 (see **Figure 2**). The TFM results match well with the experimental data and with the Ergun equation. The minimum fluidization velocities determined by experiments and TFM are 0.218 and 0.212 respectively, and match very well. The small difference between the slopes of the experimental and TFM/Ergun equation is caused by the difference between the TFM and experimental porosity at minimum fluidization velocity.

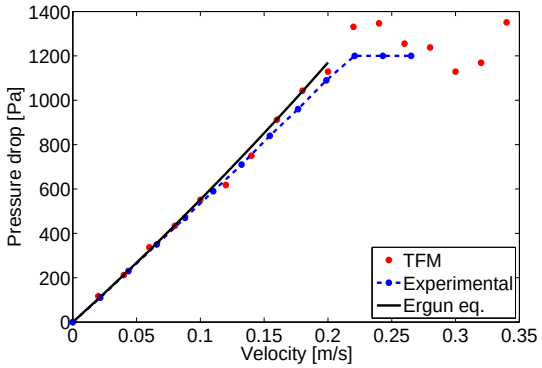

Figure 2: Pressure drop versus gas velocity for experiments, TFM simulations and Ergun equation calculations based on the TFM porosity.

Geometries and model settings

A grid sensitivity study was performed for fluidized bed membrane reactors with one membrane in the center of the bed. The flux around the membrane is not uniform and is lowest on top of the membrane. Furthermore, the time-averaged solids hold-up on top of the membranes is higher than elsewhere around the membrane, which could suggest there is a relation between the reduced flux and increased solids hold-up. Further details will be discussed in the results section.

The tested grids are displayed in **Figure 3** and are labeled coarse (28 cells counted around the circumference of the membrane), middle (64 cells) and fine (128 cells). The computed fluxes of the different grids were time-averaged over 25 seconds of simulation time and compared to each other to verify whether grid independent results were obtained. The coarse grid was not yet grid independent, whereas the middle and fine grid are relatively close to each other. The large number of grid cells in the fine grid would however require the simulations to be run at unfeasibly small time-steps, which would result in very long simulation times, especially when extending this to systems with membrane tube banks. Therefore, the middle grid was used for all further cases studied in this work.

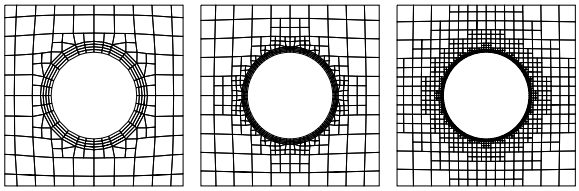

Figure 3: Grids around membranes for a coarse grid with 28 cells (left), middle grid with 64 cells (middle) and fine grid with 128 cells (right) adjacent to the membrane boundary.

Various horizontal membrane configurations were simulated. To keep practical simulation times, full 2D simulations were performed. As Asegehehn et al. (2011) reported, bubble behavior is quite similar for 2D and 3D systems with immersed tubes. The simulation settings are given in **Table 1**. The configurations and dimensions of the tube banks are presented in **Figure 4**. Configurations (a)–(d) are the base cases called Wall Membranes (WM), because membranes are present close to the bed walls. In configurations (e)–(h) the membranes closest to the walls have been removed, so they are called No Wall Membranes (NWM). In configurations (i)–(l) the membranes near the walls have been replaced with inactive tubes (portrayed as open black circles), so they are referred to as Tubes (T). The Tubes cases have the same membrane area as the No Wall Membranes cases, but the same membrane/tube locations as the Wall Membranes cases. The hydrodynamic effect that objects near the bed walls have on the system performance can hereby be quantified. The membrane tube banks have either been placed in a staggered or in an in-line configuration. The Full Staggered (FS) cases are configured in the same way as the Half Staggered (HS) cases, except they have double the number of membranes. This is also the case with the Full In-line (FI) and Half In-line (HI) configurations. Industrially, the half tube bank cases could be useful for auto-thermal reactions; the empty bottom section can be used to generate heat for the reaction by combustion. Furthermore, overloading the system with too many modern high flux membranes will result in a low performance per membrane, which would make the system less feasible.

Table 1: Summary of TFM simulation settings for all horizontal membrane cases.

Par.	Value	Par.	Value
Width	0.30 m	ρ_p	2500 kg/m^3
Height	0.90 m	D_{H_2}	$1.0 \cdot 10^{-4}$ m^2/s
$N_{c,width}$	150	Q_{pd}	$4.3 \cdot 10^{-3}$ mol/(m^{2}s Pa^n)
$N_{c,height}$	450	n	0.50
d_m	9.6 mm	T	405 °C
d_p	500 μm	$X_{H_2,in}$	0.25
e_{pp}	0.97	p_{outlet}	$1.6 \cdot 10^5$ Pa
e_{pw}	0.97	p_{perm}	$0.01 \cdot 10^5$ Pa
u/u_{mf}	3.0	t_{sim}	30 s
u_{mf}	0.21 m/s	Δt_{max}	$1 \cdot 10^{-5}$ s

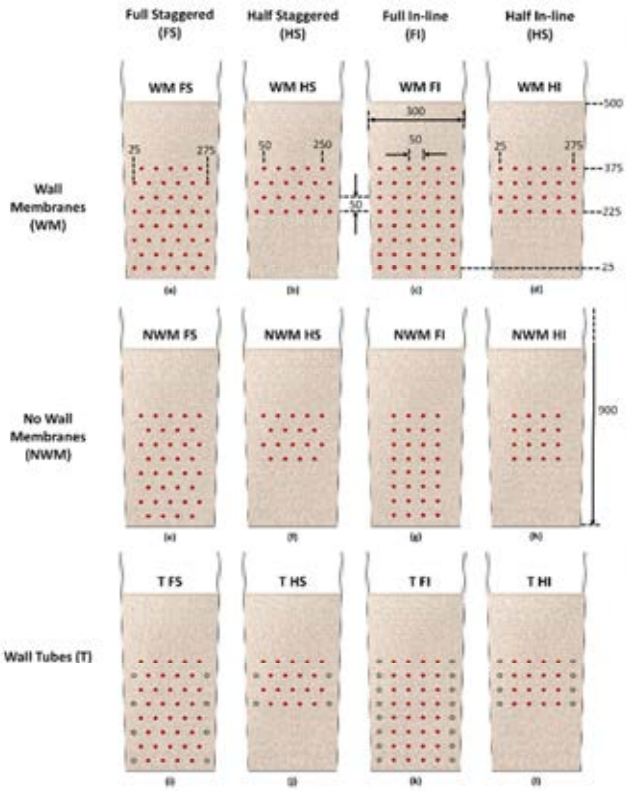

Figure 4: Membrane tube bank configurations:
Wall Membranes
(a) Full Staggered (WM FS); (b) Half Staggered (WM HS); (c) Full In-line (WM FI); (d) Half In-line (WM HI).
No Wall Membranes
(e) Full Staggered (NWM FS); (f) Half Staggered (NWM HS); (g) Full In-line (NWM FI); (h) Half In-line (NWM HI).
Wall Tubes (black open circles)
(i) Full Staggered (T FS); (j) Half Staggered (T HS); (k) Full In-line (T FI); (l) Half In-line (T HI). All given measurements are in mm.

RESULTS

Mass transfer limitations

The main mass transfer limitations in fluidized beds with horizontally immersed membranes are at the membranes located near the bed walls (**Figure 5**). The time-averaged hydrogen mole fractions are lowest on top of the membranes near the walls. For the full in-line configuration (**Figure 4 c**) the time averaged hydrogen flux of the membranes at the walls is in some cases half of the flux of the all membranes in the middle. The flux of the membranes in the middle does show a similar trend as the flux of the membranes near the walls. Mass transfer is mostly limited on top of the membranes, whereas the best performance is found at the bottom of the membranes. This flux profile can be related to hydrodynamic effects that have already been observed by Medrano et al. (2015). In their work, densified zones and gas pockets were found to be potential mass transfer limitations for horizontally immersed membranes.
In the next section, the effect of these densified zones and gas pockets on mass transfer of hydrogen towards horizontally immersed membranes will be discussed in more detail.

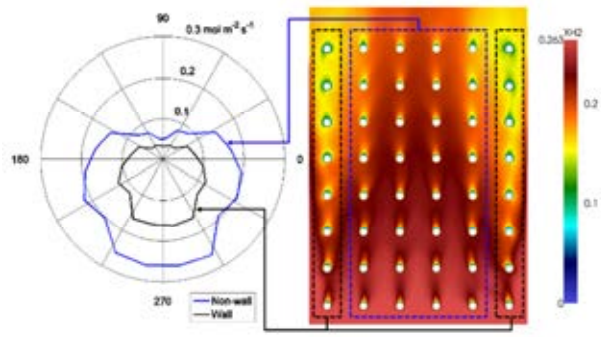

Figure 5: Time-averaged hydrogen flux at various angles around the membranes, and a snapshot of time-averaged hydrogen mole fractions, both for the full inline membrane tube bank configuration.

Densified zones, gas pockets and gas flow patterns

Gas pockets and densified zones are observed both in TFM simulations and during experiments. Gas pockets are formed because the downward movement of solids shields the underside, which can cause areas with very little solids content to form underneath the membranes. Gas pockets mostly appear near the walls, but they can be found underneath any horizontally immersed membrane.

No significant effect of gas pockets on the mass transfer towards the membranes was found. **Figure 6** shows two snapshots, one taken right before the gas pocket occurs, and one while the gas pocket is at its largest. Similar to regular bubbles in fluidized beds, the gas mixture follows the path of least resistance and therefore flows through areas with the lowest particle content, such as gas pockets. The streamlines show that the gas flowing around the membrane has a significant effect on where reduced hydrogen concentrations are observed. The gas cannot easily flow to the top of the membranes, which enables solids to accumulate here (densified zones), making it more difficult to quickly replenish hydrogen here.

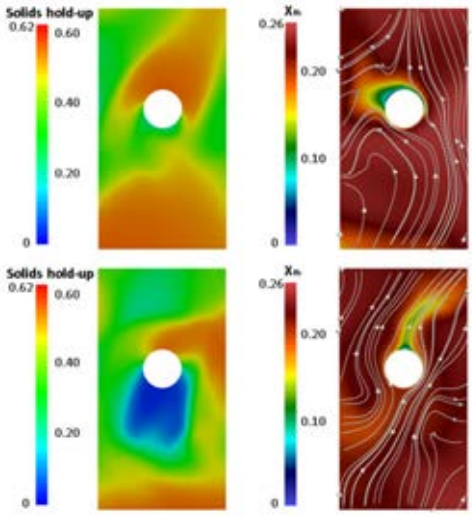

Figure 6: Snapshot of the solids hold-up, hydrogen mole fraction and gas velocity streamlines around a horizontally immersed membrane with and without a gas pocket.

Densified zones can be present on top of membranes anywhere in the reactor. Similar to gas pockets, they mostly occur at the membranes that are located near the bed walls, because the solids flow downwards onto the top of the membranes there. Next to solids down flow, **Figure 7** shows that an important reason for densified zones to form is that gas cannot easily reach the top of the membranes. The gas velocities are especially low near the membranes close to the walls. Because of the no-slip behavior of the gas near the walls, the gas has insufficient momentum to move the downward flowing solids away from the membranes near the walls. In the middle of the reactor, less densified zones are present, but they still occur because the gas cannot always reach the top of the membrane easily.

The time-averaged hydrogen mole fractions in **Figure 7** show that densified zones have a detrimental effect on mass transfer towards the membrane. On top of the membrane, the hydrogen mole fractions (thus also the hydrogen fluxes) are significantly lower compared to elsewhere around the membrane. The effect is mostly noticeable near the walls, where clearly some gas back-mixing is visible, but also in the middle of the reactor a reduced hydrogen flux was observed on top of the membrane. This is intrinsic to the way the membranes are placed compared to the flow direction. the gas cannot always reach the top of the membrane easily, because the membrane itself shields the top-side of the membrane. In **Figure 5** this is visible, because the time-averaged hydrogen flux is also lower on top of the membranes in the middle.

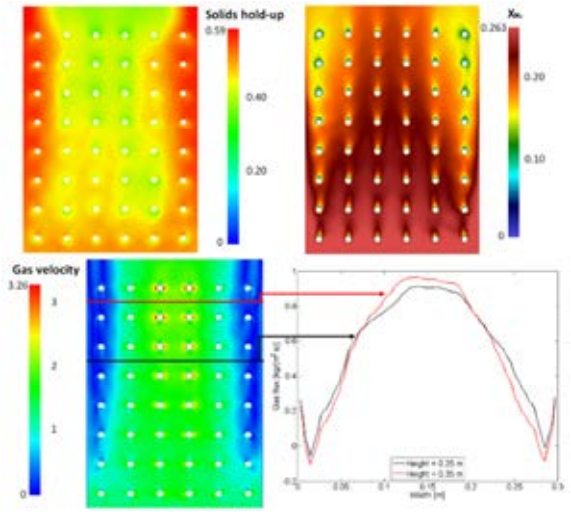

Figure 7: Snapshot of the time-averaged solids hold-up, hydrogen mole fractions and gas velocities (in m/s) in a fluidized bed with a full in-line membrane tube bank.

Effect of tube bank configuration on hydrogen flux

The main mass transfer limitations towards the membranes have already been identified near the bed walls. This section will quantify how much the mass transfer limitations affect the flux for various membrane tube bank configurations. **Figure 8** and **Figure 9** present the time-averaged hydrogen flux profiles at various width positions and various angles around the membranes for all the full in-line and half in-line configurations from **Figure 4**. The membranes near the

walls perform approximately three to five times worse than the membranes in the middle of the reactor for the full and half in-line configurations. Adding inert tubes near the walls does not have a significant effect on the system performance. The polar plots in **Figure 8** and **Figure 9** show that when active membranes are placed close to the walls, the averaged flux of all membranes is reduced. The in-line configurations with half tube banks show similar behavior to the full tube bank configurations.

In general, the flux over the reactor width in the full staggered configurations is more equal over the width than in the full in-line one (see **Figure 10)**. However, some of the membranes that have not been removed in the full staggered configuration still have reduced flux, even though the difference between the highest and the lowest flux is about a factor two. In general the results show that membranes that are approximately within 8 cm distance of the walls (about 20% of the total bed width) suffer from reduced flux. Because bubbles cannot channel through the staggered membrane tube banks, the membranes near the walls perform better in a staggered configuration than in an in-line one. The flux is slightly higher for the membranes in the middle of the half tube bank configurations, because in the full tube bank configurations a lot of the hydrogen has already been extracted before it reaches the membranes in the top of the tube bank, which results in lower fluxes for the top membranes.

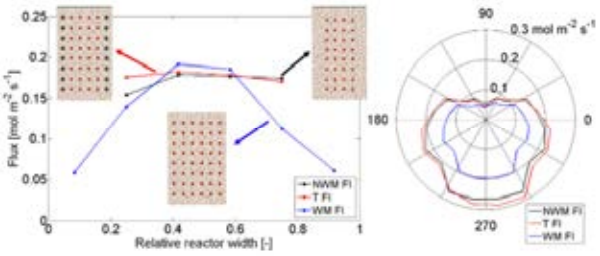

Figure 8: Time-averaged flux for the full in-line tube bank configurations without wall membranes, with inert tubes at the walls and with wall membranes; (left) flux versus relative reactor width (right) flux averaged over all membranes at various angles around the membranes.

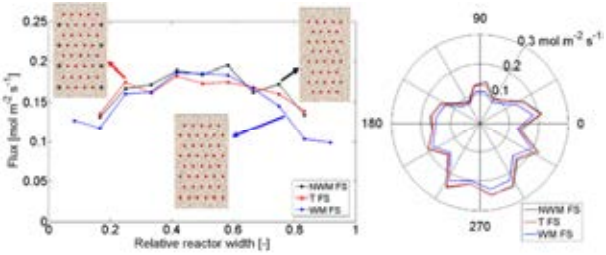

Figure 9: Time-averaged flux for the full staggered tube bank configurations without wall membranes, with inert tubes at the walls and with wall membranes; (left) flux versus relative reactor width (right) flux averaged over all membranes at various angles around the membranes.

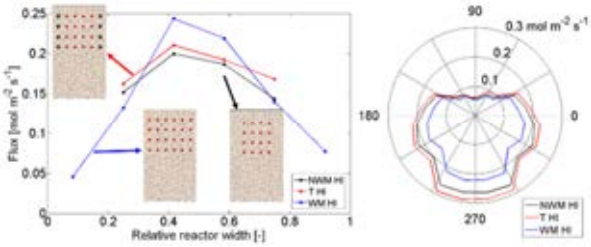

Figure 10: Time-averaged flux for the half in-line tube bank configurations without wall membranes, with inert tubes at the walls and with wall membranes; (left) flux versus relative reactor width (right) flux averaged over all membranes at various angles around the membranes.

CONCLUSION

The performance of fluidized bed membrane reactors with various horizontally immersed membrane tube bank configurations was investigated. The flux is lowest at the top of the membranes and highest below the membranes. The densified zones and the gas flow patterns have a significant negative effect on the hydrogen permeation flux. Gas pockets have no negative effect on the mass transfer from the emulsion phase to the membrane. However, gas pockets could reduce the reaction rate of systems in which the extracted product is produced via a catalytic reaction.

In systems with tube banks, membranes that are placed close to the fluidized bed walls show significantly lower performance than the membranes in the center of the bed. The down flowing solids and reduced gas flow near the walls keeps the flux low here. Replacing the wall membranes with inactive tubes does not have a significant positive effect on the system, so removal of the wall membranes is therefore advised. In case of exothermal or endothermal reactions, wall tubes can perhaps be used for internal cooling or heating.

Future work on fluidized beds with horizontally immersed membranes should focus on methods to reduce the mass transfer limitations towards the membranes. Potential methods include having a non-uniform gas feed, pulsating gas inlet flow rate, changing the membrane pitch and using as large as possible particles to increase the dispersion effects.

ACKNOWLEDGEMENTS

The authors are grateful to TTW and NWO for their financial support through the VIDI project ClingCO_2, project number 12365.

REFERENCES

ADRIS, A.M., LIM, C.J. and GRACE, J.R., (1994), "The fluidized bed membrane reactor system: a pilot scale experimental study", *Chem. Eng. Sc.*, **49**, 5833-5843.

ASEGEHEGN, T.W., SCHREIBER, M. and KRAUTZ, H.J., (2011), "Numerical simulation and experimental validation of bubble behavior in 2D gas–solid fluidized beds with immersed horizontal tubes", *Chem. Eng. Sc.*, **66**, 5410-5427.

CARAVELLA, A., BARBIERI, G. and DRIOLI, E., (2009), "Concentration polarization analysis in self-

supported Pd-based membranes", *Purif. Technol.,* **66**, 613-624.

CORONEO, M., MONTANTE, G., CATALANO, J. and PAGLIANTI, A., (2009), "Modelling the effect of operating conditions on hydrodynamics and mass transfer in a Pd-Ag membrane module for H_2 purification", *J. Memb. Sc.*, **343**, 34-41.

DANG, T.Y.N., GALLUCCI, F. and VAN SINT ANNALAND, M., (2014), "Micro-structured fluidized bed membrane reactors: solids circulation and densified zones distribution", *Chem. Eng. J.*, **239**, 42-52.

DE JONG, J.F., VAN SINT ANNALAND, M. and KUIPERS, J.A.M., (2011), "Experimental study on the effects of gas permeation through flat membranes on the hydrodynamics in membrane-assisted fluidized beds", *Chem. Eng. Sc.*, **66**, 2398-2408.

DE JONG, J.F., VAN SINT ANNALAND, M. and KUIPERS, J.A.M., (2012), "Membrane-assisted fluidized beds - part 2: numerical study on the hydrodynamics around immersed gas-permeating membrane", *Chem. Eng. Sc.*, **84**, 822-833.

ERGUN, S. and ORNING, A., (1949), "Fluid flow through randomly packed columns and fluidized beds", *Ind. Eng. Chem.*, **41**, 1179-1184.

GALLUCCI, F., VAN SINT ANNALAND, M. and KUIPERS, J.A.M., (2008), "Autothermal reforming of methane with integrated CO_2 capture in a novel fluidized bed membrane reactor. Part 1: experimental demonstration", *Top. Catal.*, **51**, 133-145.

GIDASPOW, D., (1994), "Multiphase flow and fluidization: continuum and kinetic theory descriptions", *Academic Press Inc.*

HOMMEL, R., Cloete, S. and AMINI, S., (2012), "Numerical investigations to quantify the effect of horizontal membranes on the performance of a fluidized bed reactor", *Int. J. Chem. Reac. Eng.*, **10**.

HELMI, A., FERNANDEZ, E., MELENDEZ, J., PACHECO TANAKA, D.A., GALLUCCI, F. and VAN SINT ANNALAND, M., (2016), "Fluidized Bed Membrane Reactors for Ultra Pure H_2 Production - A Step forward towards Commercialization", *Molecules*, **21**, 376.

HELMI, A., VONCKEN, R.J.W., RAIJMAKERS, T., ROGHAIR, I., GALLUCCI, F., and VAN SINT ANNALAND, M., (2017), "On concentration polarization in fluidized bed membrane reactors", *Submitted to Chem. Eng. J.*.

JOHNSON, P.C. and JACKSON, R., (1987), "Frictional-collisional constitutive relations for granular materials, with application to plane shearing", *J. Fluid Mech.*, **176**, 67–93.

KUIPERS, J.A.M., VAN DUIN, K.J., VAN BECKUM, F.P.H., and VAN SWAAIJ, W.P.M., (1992), "A numerical model of gas-fluidized beds", *Chem. Eng. Sci.*, **47**, 1913–1924.

LIU, Y. and HINRICHSEN, O., (2014), "CFD modeling of bubbling fluidized beds using OpenFOAM®: Model validation and comparison of TVD differencing schemes", *Comp. & Chem. Eng.*, **69**, 75-88.

LUN, C.K.K., SAVAGE, S.B., JEFFREY, D.J., and CHEPURNIY, N., (1984), "Kinetic theories for granular flow: inelastic particles in Couette flow and slightly inelastic particles in a general flowfield", *J. Fluid Mech.*, **140**, 223-256.

MA, D. and AHMADI, G., (1988), "A kinetic model for rapid granular flows of nearly elastic particles including interstitial fluid effects", *Powder Technol.*, **56**, 191-207.

MEDRANO, J.A., SPALLINA, V., VAN SINT ANNALAND, M. and GALLUCCI, F., (2014), "Thermodynamic analysis of a membrane-assisted chemical looping reforming reactor concept for combined H_2 production and CO_2 capture", *Int. J. Hydrogen Energy*, **39**, 4725-4738.

MEDRANO, J.A., VONCKEN, R.J.W., ROGHAIR, I., GALLUCCI, F. and VAN SINT ANNALAND, M., (2015), "On the effect of gas pockets surrounding membranes in fluidized bed membrane reactors: An experimental and numerical study", *Chem. Eng. J.*, **282**, 45-57.

MLECZKO, L., OSTROWSKI, T. and WURZEL, T., (1996), "A fluidised-bed membrane reactor for the catalytic partial oxidation of methane to synthesis gas", *Chem. Eng. Sc.*, **51**, 3187-3192.

MOHSEN, M.F.N. and BALUCH, M.H., (1983), "An analytical solution of the diffusion-convection equation over a finite domain", *Appl. Math. Model.*, **7**, 285-287.

NIEUWLAND, J.J., VAN SINT ANNALAND, M., KUIPERS, J.A.M. and VAN SWAAIJ, W.P.M, (1996), "Hydrodynamic modeling of gas/particle flows in riser reactors", *AIChE J.*, **42**, 1569-1582.

PASSALACQUA, A. and FOX, R.O., (2011), "Implementation of an iterative solution procedure for multi-fluid gas-particle flow models on unstructured grids", *Powder Technol.*, **213**, 174-187.

RONG, D., MIKAMI, T. and HORIO, M., (1999), "Particle and bubble movements around tubes immersed in fluidized beds – a numerical study", *Chem. Eng. Sc.*, **54**, 5737-5754.

RUSCHE, H., (2002), "Computational fluid dynamics of dispersed two-phase flows at high phase fractions", PhD thesis, *University of London*.

SRIVASTAVA, A. and SUNDARESAN, S., (2003), "Analysis of a frictional-kinetic model for gas-particle flow", *Powder Technol.*, **129**, 72-85.

SARKAR, A., SUN, X. and SUNDARESAN, S., (2013), "Sub-grid drag models for horizontal cylinder arrays immersed in gas-particle multiphase flows", *Chem. Eng. Sc.*, **104**, 399-412.

SOLNORDAL, C.B., KENCHE, V., HADLEY, T.D., FENG, Y., WITT, P.J. and LIM, K.-S., (2015), "Simulation of an internally circulating fluidized bed using a multiphase particle-in-cell method", *Powder Technol.*, **274**, 123-134.

WANG, Q., YANG, H., FENG, Y., WITT, P.J., LU, J. and YIN, W., (2015), "Numerical study of the effect of operation parameters on particle segregation in a coal beneficiation fluidized bed by a TFM-DEM hybrid model", *Chem. Eng. Sc.*, **131**, 256-270.

YANG, S., LUO, K., FANG, M., FAN, J and CEN, K., (2014), "Discrete element study of solid circulating and resident behaviors in an internally circulating fluidized bed", *Chem. Eng. J.*, **248**, 145-157.

TAN, L., ROGHAIR, I. and VAN SINT ANNALAND, M., (2014), "Simulation study on the effect of gas permeation on the hydrodynamic

characteristics of membrane-assisted micro fluidized beds", ***Appl. Math. Model.***, **38**, 4291-4307.

TIEMERSMA, T.P., PATIL, C.S., VAN SINT ANNALAND, M. and KUIPERS, J.A.M., (2006), "Modelling of packed bed membrane reactors for autothermal production of ultrapure hydrogen", ***Chem. Eng. Sc.***, **61**, 1602-1616.

TSOTSIS, T.T., CHAMPAGNIE, A.M., VASILEIADIS, S.P., ZIAKA, Z.D. and MINET, R.G., (1992), "Packed bed catalytic membrane reactors", ***Chem. Eng. Sc.***, **47**, 2903-2908.

VAN DER HOEF, M.A., YE, M., VAN SINT ANNALAND, M., ANDREWS IV, A.T., SUNDARESAN, S. and KUIPERS, J.A.M., (2006) "Multi-scale modeling of gas-fluidized beds", ***Adv. Chem. Eng.*** **31**, 65–149.

VAN WACHEM, B.G.M., (2000), "Derivation, implementation, and validation of computer simulation models for gas-solid fluidized beds", PhD thesis, Delft University of Technology.

VONCKEN, R., ROGHAIR, I., GALLUCCI, F. and VAN SINT ANNALAND, M., (2015), "Mass transfer phenomena in fluidized beds with vertically and horizontally immersed membranes", ***Proc. 11th Int. Conf. Comput. Fluid Dyn. Miner. Process Ind. (CFD 2015)***, 031VON 1-6.

WASSIE, S.A., GALLUCCI, F., CLOETE, S., ZAABOUT, A., VAN SINT ANNALAND, M., and AMINI, S., (2015), "The effect of gas permeation through vertical membranes on chemical switchting reforming (CSR) reactor performance", ***Int. J. Hydrogen Energy***, **41**, 8640-8655.

WEN, C. and YU, Y., (1966) "A generalized method for predicting the minimum fluidization velocity" ***AICHEJ.*** **12**, 610-612.

WHITE, F.M., (1991), "Viscous fluid flow", ***McGraw-Hill Inc***.